Inorganic Chemistry

Article

pubs.acs.org/IC

Synthesis, Structural Characterization, and Electrochemical Properties of Dinuclear Ni/Mn Model Complexes for the Active Site of [NiFe]-Hydrogenases

Li-Cheng Song,* Jia-Peng Li, Zhao-Jun Xie, and Hai-Bin Song

Department of Chemistry, State Key Laboratory of Elemento-Organic Chemistry, Nankai University, Tianjin 300071, China

Supporting Information

ABSTRACT: Four new dinuclear Ni/Mn model complexes $RN(PPh_2)_2Ni(\mu\text{-}SEt)_2(\mu\text{-}Cl)Mn(CO)_3$ (**7**, R = *p*-$MeC_6H_4CH_2$; **8**, R = EtO_2CCH_2) and $RN(PPh_2)_2Ni(\mu\text{-}SEt)_2(\mu\text{-}Br)Mn(CO)_3$ (**9**, R = *p*-$MeC_6H_4CH_2$; **10**, R = EtO_2CCH_2) have been prepared via the four separated step-reactions involving six new precursors $RN(PPh_2)_2$ (**1**, R = *p*-$MeC_6H_4CH_2$; **2**, R = EtO_2CCH_2), $RN(PPh_2)_2NiCl_2$ (**3**, R = *p*-$MeC_6H_4CH_2$; **4**, R = EtO_2CCH_2), and $RN(PPh_2)_2Ni(SEt)_2$ (**5**, R = *p*-$MeC_6H_4CH_2$; **6**, R = EtO_2CCH_2). The Et_3N-assisted aminolysis of Ph_2PCl with *p*-$MeC_6H_4CH_2NH_2$ or $EtO_2CCH_2NH_2{\cdot}HCl$ in CH_2Cl_2 gave the azadiphosphine ligands **1** and **2** in 38% and 53% yields, whereas the coordination reaction of **1** or **2** with $NiCl_2{\cdot}6H_2O$ in CH_2Cl_2/MeOH afforded the mononuclear Ni dichloride complexes **3** and **4** in 59% and 78% yields, respectively. While thiolysis of **3** or **4** with EtSH under the assistance of Et_3N in CH_2Cl_2 produced the mononuclear Ni dithiolate complexes **5** and **6** in 64% and 68% yields, further treatment of **5** and **6** with $Mn(CO)_5Cl$ or $Mn(CO)_5Br$ resulted in formation of the dinuclear Ni/Mn model complexes **7**−**10** in 31−73% yields. All the new compounds **1**−**10** have been structurally characterized, while model complexes **7** and **9** have been found to be catalysts for HOAc proton reduction to hydrogen under CV conditions.

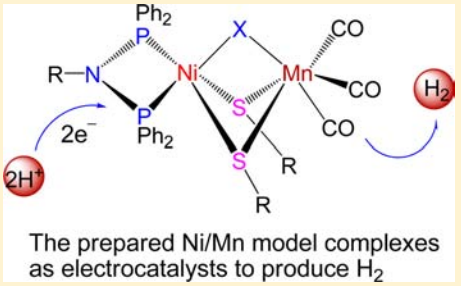

INTRODUCTION

Hydrogenases are natural enzymes that can reversibly catalyze the hydrogen metabolism in a variety of microorganisms.[1,2] According to the metal content in their active sites, hydrogenases are mainly divided into three groups: [FeFe]-hydrogenases,[3,4] [NiFe]-hydrogenases,[5,6] and [Fe]-hydrogenase (Hmd).[7,8] X-ray crystallographic study revealed that the active site of [NiFe]-hydrogenases isolated from *D. gigas*, *D. vulgaris Miyazaki F*, and *Dm. baculatum*[9−12] exists as two states. One is the oxidized state in which the metal Ni and Fe centers are bridged by two cysteine S atoms and one hydroxyl O atom. The other is a reduced state in which the Ni and Fe centers are bridged by two cysteine S atoms or perhaps with an additional H-bridge. Although the two active site structures have some differences, they both consist of a butterfly $[NiS_2Fe]$ cluster core, in which the Fe center is coordinated by one terminal CO and two terminal CN^- ligands, and the Ni center is coordinated by two terminal cysteine Cys−S ligands (an exception is for *Dm. baculatum* in which its Ni atom is coordinated by one terminal Cys-S ligand and one terminal seleno-cysteine Cys-Se ligand); in addition, the two metal centers are combined together by two bridging Cys−S ligands (Figure 1a).[9−14]

Under the guidance of such well-elucidated active site structures, synthetic chemists have designed and synthesized many heteronuclear transition-metal complexes as useful models for the active site of [NiFe]-hydrogenases, such as the heteronuclear Ni/Fe,[15−28] Ni/Ru,[29−34] and Ni/Mn model complexes.[35,36] As part of our research project related to [NiFe]-hydrogenases,[37,38] we recently launched a study aimed to synthesize the new type of Ni/Mn model complexes in which a $Mn^{+I}(CO)_3$ moiety is combined with an azadiphosphine $(Ph_2P)_2NR$-chelated Ni center via two bridging thiolate ligands and one bridging halide ligand (Figure 1b). The reasons we are interested in preparing such a type of model complexes are the following: (i) Only one Ni/Mn model complex, namely the cationic type of complex $[Ni(xbsms)Mn(CO)_3(H_2O)]^+Br^-$, has so far been prepared by two methods.[35,36] (ii) The $Mn^{+I}(CO)_3$ (d^6ML_3) fragment in our designed target model complexes is isolobal with the $Fe^{+II}(CO)(CN)_2$ (d^6ML_3) moiety[39] found in the active site of [NiFe]-hydrogenases, and thus, such complexes might have the structures and some properties similar to the active site of the natural enzymes. (iii) The azadiphosphine 1,3,6-triphenyl-1-aza-3,6-diphosphacycloheptane-chelated mononuclear Ni complex, which contains a pendant amine N atom in its azadiphosphine ligand, is known to be able to catalyze proton reduction to hydrogen at remarkable rates.[40] Fortunately, we have successfully prepared such a new type of Ni/Mn model complexes with a general formula $RN(PPh_2)_2Ni(\mu\text{-}SEt)_2(\mu\text{-}X)Mn(CO)_3$ (Figure 1b, R = *p*-$MeC_6H_4CH_2$, EtO_2CCH_2; X = Cl, Br). Now, we wish to report the synthesis, structural characterization, and some electrochemical properties of the

Received: July 31, 2013
Published: September 24, 2013

dx.doi.org/10.1021/ic401978h | *Inorg. Chem.* 2013, 52, 11618−11626

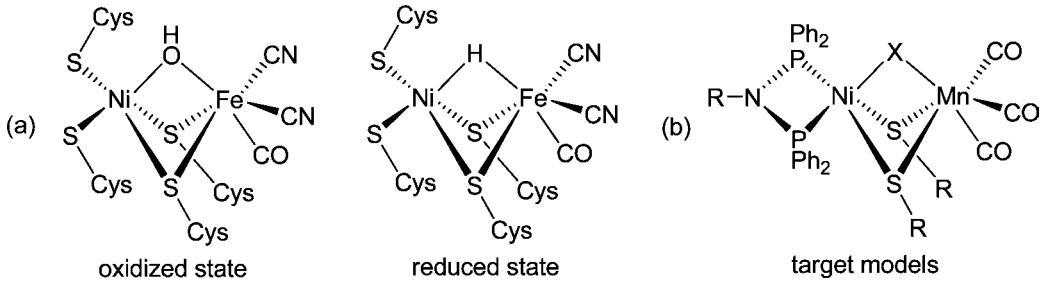

Figure 1. (a) Oxidized and reduced states of the active site of [NiFe]-hydrogenases determined by protein X-ray crystallography. (b) Target Ni/Mn model complexes.

Scheme 1

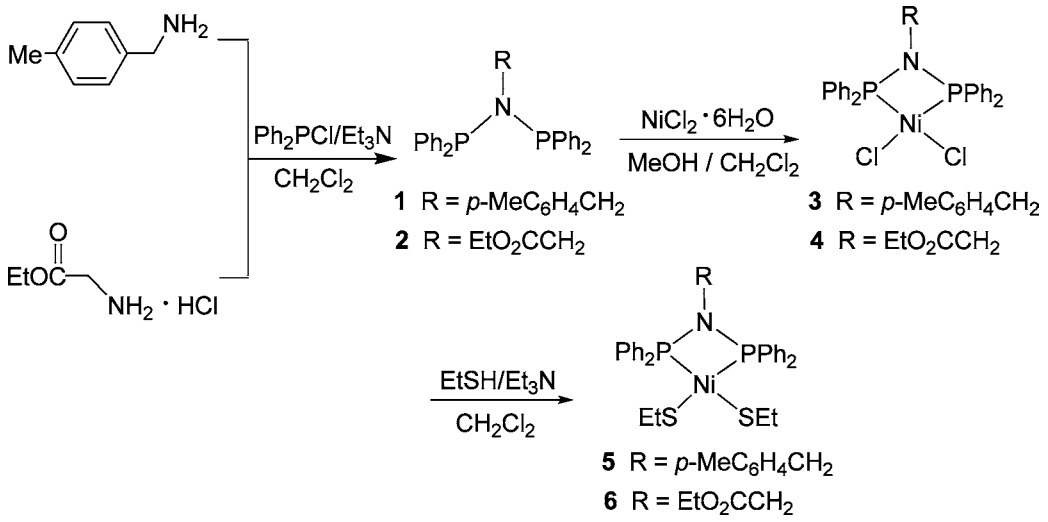

new type of Ni/Mn model complexes along with the new precursors used for their preparation.

RESULTS AND DISCUSSION

Synthesis and Characterization of Azadiphosphine Ligands $RN(PPh_2)_2$ (1, R = *p*-$MeC_6H_4CH_2$; 2, R = EtO_2CCH_2) and Mononuclear Ni Complexes $RN(PPh_2)_2NiCl_2$ (3, R = *p*-$MeC_6H_4CH_2$; 4, R = EtO_2CCH_2)/ $RN(PPh_2)_2Ni(SEt)_2$; 5, R = *p*-$MeC_6H_4CH_2$; 6, R = EtO_2CCH_2). According to our designed synthetic route to the target Ni/Mn model complexes $RN(PPh_2)_2Ni(SEt)_2(\mu\text{-}X)Mn(CO)_3$ (7–**10**, R = *p*-$MeC_6H_4CH_2$, EtO_2CCH_2; X = Cl, Br), we should first prepare the new precursor compounds **1**–**6**. As shown in Scheme 1, (i) the azadiphosphine ligands **1** and **2** could be simply prepared by aminolysis of Ph_2PCl with *p*-methylbenzylamine or glycine ethyl ester hydrochloride in CH_2Cl_2 in the presence of excess Et_3N from 0 °C to room temperature in 38% and 53% yields, respectively; (ii) the mononuclear Ni dichloride complexes **3** and **4** were prepared by coordination reaction of azadiphosphine ligand **1** or **2** with $NiCl_2{\cdot}6H_2O$ in CH_2Cl_2/MeOH at room temperature in 59% and 78% yields, respectively; and (iii) thiolysis of the mononuclear Ni dichlorides **3** and **4** with EtSH in the presence of excess Et_3N in CH_2Cl_2 at room temperature gave rise to the mononuclear Ni dithiolates **5** and **6** in 64% and 68% yields, respectively.

All precursors **1**–**6** are air-stable solids, which have been characterized by elemental analysis and various spectroscopic methods. The IR spectra of **1**–**6** showed one strong absorption band in the range 808–835 cm^{-1} for the stretching vibration of the P–N–P skeleton in the free and coordinated azadiphosphine ligands.[41] The ^1H and ^{13}C NMR spectra of **1**–**6** displayed the corresponding signals for their organic groups. The ^{31}P NMR spectra of **1**–**6** each exhibited one singlet in the region 46–65 ppm for their two chemically equivalent phosphorus atoms.

Although the crystal structures of precursors **4**–**6** were not obtained due to lack of suitable single crystals, we have determined the crystal structures of precursors **1**–**3** by X-ray diffraction analysis. The ORTEP plots of **1** and **2** are shown in Figures 2 and 3, whereas Table 1 lists their selected bond lengths and angles. As shown in Figures 2 and 3, the two azadiphosphine ligands **1** and **2** each contain one $(Ph_2P)_2N$ unit that is respectively attached to *p*-$MeC_6H_4CH_2$ and EtO_2CCH_2 groups via its N atom. The bond lengths N1–P1 (1.7176 Å)/N1–P2 (1.7247 Å) and bond angle ∠P1–N1–P2 (122.55°) for **1** are very close to the corresponding those of **2** (1.7198 Å/1.7174 Å and 124.17°, respectively) and are comparable with those reported for similar compounds.[42,43] Figure 4 shows the ORTEP plot of mononuclear Ni complex **3**, whereas Table 2 lists its selected bond lengths and angles. As can be seen in Figure 4, the azadiphosphine ligand **1** is chelated via P1 and P2 atoms to Ni1 atom with two terminal chloro ligands. The central metal Ni1 atom adopts a slightly distorted square-planar coordination geometry, which is reflected by the observation that the dihedral angle between the two triangular planes involving P1/Ni1/P2 atoms and Cl1/Ni1/Cl2 atoms is only 3.52°. The four-membered metallacycle P1Ni1P2N1 is also nearly planar since the dihedral angle between the two

dx.doi.org/10.1021/ic401978h | *Inorg. Chem.* 2013, 52, 11618–11626

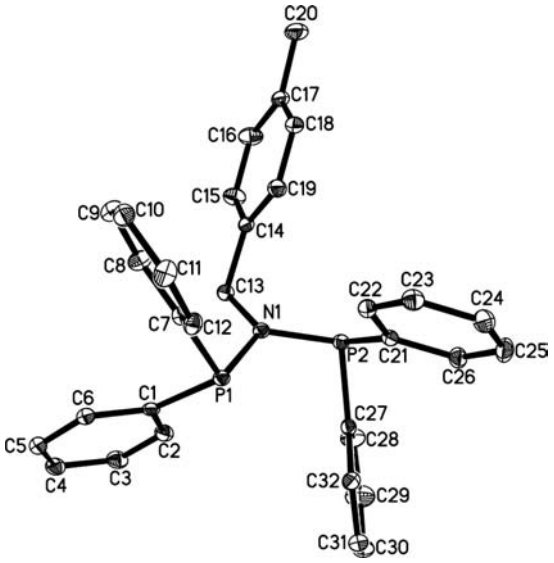

Figure 2. Molecular structure of **1** with 30% probability level ellipsoids. Hydrogen atoms are omitted for clarity.

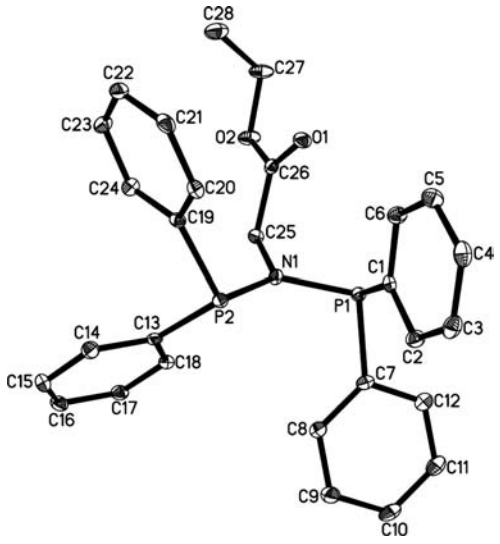

Figure 3. Molecular structure of **2** with 30% probability level ellipsoids. Hydrogen atoms are omitted for clarity.

triangular planes involving P1/Ni1/P2 atoms and P1/N1/P2 atoms is only 3.67°. The bond lengths Ni1−P1 (2.1261 Å), Ni1−Cl1 (2.1914 Å), and N1−P1 (1.693 Å) are very close to those of Ni1−P2 (2.1354 Å), Ni1−Cl2 (2.2152 Å), and N1−P2 (1.697 Å), respectively. The bond angles ∠Cl1−Ni1−Cl2, ∠P1−Ni1−P2, and ∠P1−N1−P2 are 98.68°, 73.70°, and 97.86°, respectively. These values are comparable with those previously reported for other similar compounds.[42,44]

Synthesis and Characterization of Dinuclear Ni/Mn Model Complexes $RN(PPh_2)_2Ni(\mu\text{-}SEt)_2(\mu\text{-}Cl)Mn(CO)_3$ (7, R = $p\text{-}MeC_6H_4CH_2$; 8, R = EtO_2CCH_2) and $RN(PPh_2)_2Ni(\mu\text{-}SEt)_2(\mu\text{-}Br)Mn(CO)_3$ (9, R = $p\text{-}MeC_6H_4CH_2$; 10, R = EtO_2CCH_2). After the precursor compounds **1**−**6** had been prepared and structurally characterized, we started to study how we could prepare the target Ni/Mn model complexes **7**−**10**. Fortunately, we found that when the mononuclear Ni dithiolates **5** and **6** were treated with an equimolar $Mn(CO)_5Cl$ or $Mn(CO)_5Br$ in dichloromethane at room temperature, the

Table 1. Selected Bond Lengths [Å] and Angles [deg] for Ligands 1 and 2

1			
P(1)−N(1)	1.7176(14)	N(1)−C(13)	1.485(2)
P(1)−C(1)	1.8314(18)	P(2)−C(21)	1.8234(18)
P(1)−C(7)	1.8410(17)	P(2)−C(27)	1.8356(17)
P(2)−N(1)	1.7247(14)	C(1)−C(2)	1.402(2)
N(1)−P(1)−C(1)	102.42(7)	N(1)−P(2)−C(27)	106.18(7)
N(1)−P(1)−C(7)	105.06(7)	C(21)−P(2)−C(27)	100.71(8)
C(1)−P(1)−C(7)	102.28(7)	C(13)−N(1)−P(1)	122.39(11)
N(1)−P(2)−C(21)	104.61(7)	P(1)−N(1)−P(2)	122.55(8)
2			
P(1)−N(1)	1.7198(13)	O(1)−C(26)	1.2004(18)
P(1)−C(1)	1.8340(15)	P(2)−C(19)	1.8300(16)
P(1)−C(7)	1.8380(15)	P(2)−C(13)	1.8323(17)
P(2)−N(1)	1.7174(13)	N(1)−C(25)	1.4550(19)
N(1)−P(1)−C(1)	104.82(6)	N(1)−P(2)−C(13)	102.70(6)
N(1)−P(1)−C(7)	106.18(7)	C(19)−P(2)−C(13)	100.65(7)
C(1)−P(1)−C(7)	101.25(7)	C(25)−N(1)−P(1)	114.00(9)
N(1)−P(2)−C(19)	104.41(7)	P(2)−N(1)−P(1)	124.17(7)

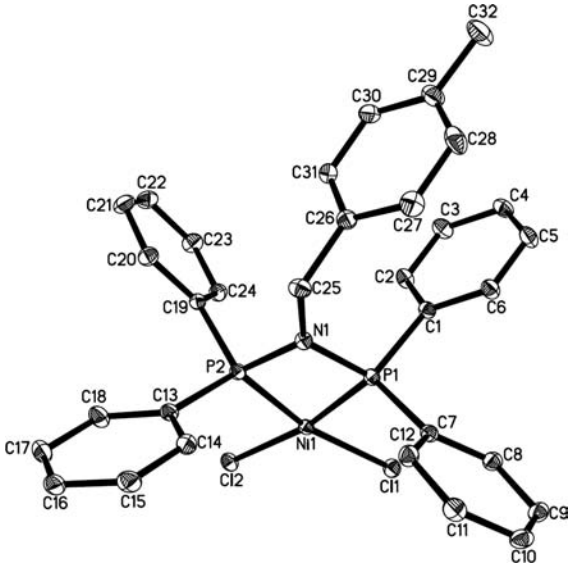

Figure 4. Molecular structure of **3** with 30% probability level ellipsoids. Hydrogen atoms are omitted for clarity.

Table 2. Selected Bond Lengths [Å] and Angles [deg] for Complex 3

Ni(1)−P(1)	2.1261(11)	P(1)−C(1)	1.811(3)
Ni(1)−P(2)	2.1354(11)	P(2)−N(1)	1.697(3)
Ni(1)−Cl(1)	2.1914(13)	P(2)−C(13)	1.801(3)
Ni(1)−Cl(2)	2.2152(11)	P(1)−N(1)	1.693(3)
P(1)−Ni(1)−P(2)	73.70(4)	N(1)−P(1)−P(2)	41.14(10)
P(1)−Ni(1)−Cl(1)	91.25(4)	N(1)−P(2)−P(1)	41.01(9)
Cl(1)−Ni(1)−Cl(2)	98.68(4)	N(1)−P(2)−Ni(1)	93.93(10)
N(1)−P(1)−Ni(1)	94.39(10)	P(1)−N(1)−P(2)	97.86(15)

target Ni/Mn complexes **7**−**10** were produced via CO substitution of $Mn(CO)_5X$ (X = Cl, Br) followed by coordination of its X ligand with Ni atom in 31−73% yields (Scheme 2).

Model complexes **7**−**10** are air-stable solids, which have been characterized by elemental analysis and spectroscopy, and, particularly for **7**, **9**, and **10**, by X-ray crystallography. For

dx.doi.org/10.1021/ic401978h | *Inorg. Chem.* 2013, 52, 11618−11626

Scheme 2

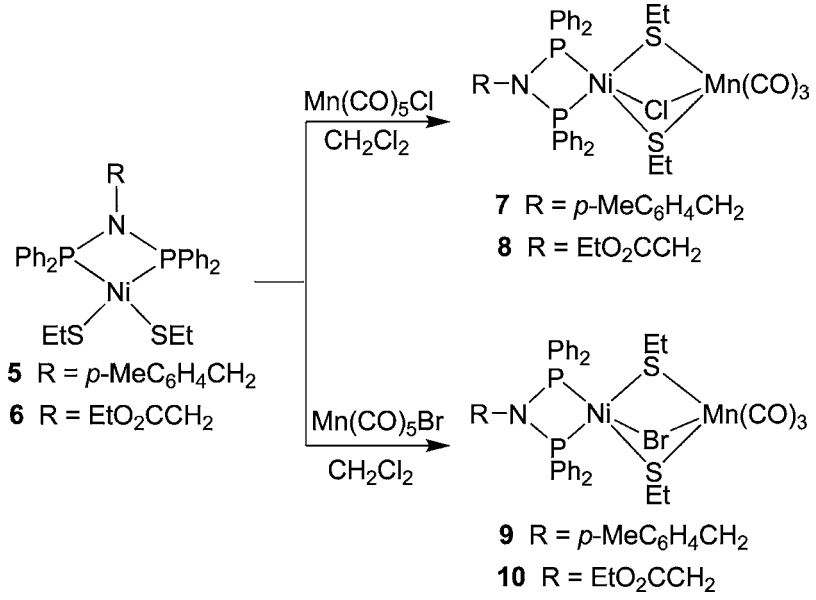

example, the IR spectra of **7**−**10** exhibited two or three absorption bands in the range 1883−2004 cm^{-1} for their terminal carbonyls and one absorption band in the region 813−818 cm^{-1} for the stretching vibration of the P−N−P skeleton in their azadiphosphine ligands.[41] The ^{1}H and ^{13}C NMR spectra showed the corresponding signals for their organic groups. In addition, the ^{31}P NMR spectra of **7**−**10** displayed one singlet in the range 45−54 ppm for their two chemically equivalent phosphorus atoms.

The X-ray crystallographic study has confirmed the molecular structures of model complexes **7**, **9**, and **10** (Figures 5−7, Table 3). Since the three Ni/Mn complexes are isostructural, we just discuss the crystal structure of complex **9**. As is shown in Figure 6, complex **9** is a dinuclear Ni/Mn complex. While the metal Ni1 atom is in a distorted square-pyramidal coordination geometry formed by P1, P2, S1, S2, and Br1 atoms with the Br1 atom occupying the apical position, the metal Mn1 atom is in a distorted octahedral coordination geometry formed by Br1, S2, C1, C2, S1, and C3 atoms with the S1 and C3 atoms positioned at the two apical positions. In addition, it is worth pointing out that (i) the distorted bond angles ∠Br1−Ni1−S1 and ∠C3−Mn1−S1 are equal to 82.67° and 170.71°, respectively; (ii) there are two bridging thiolates and one bridging bromo ligand between the Ni1 and Mn1 metal centers; and (iii) the Ni1−Mn1 distance is 3.0722 Å, which is close to that (2.8−2.9 Å) found in the oxidized state of [NiFe]-hydrogenases but considerably longer than that (2.5−2.6 Å)[10,11] found in the reduced state of [NiFe]-hydrogenases. Although the crystal structure of the first Ni/Mn model complex $[Ni(xbsms)Mn(CO)_3(H_2O)]^+Br^-$ was not determined, the DFT calculations indicated that its Ni−Mn distance is 3.152 Å,[36] which is somewhat longer than those of **7** (3.0540 Å), **9** (3.0722 Å), and **10** (3.0600 Å) determined by X-ray crystallography. Apparently, the short metal−metal distances for our Ni−Mn model complexes are due to the fact that the two metal centers in **7**−**10** are triply bridged.

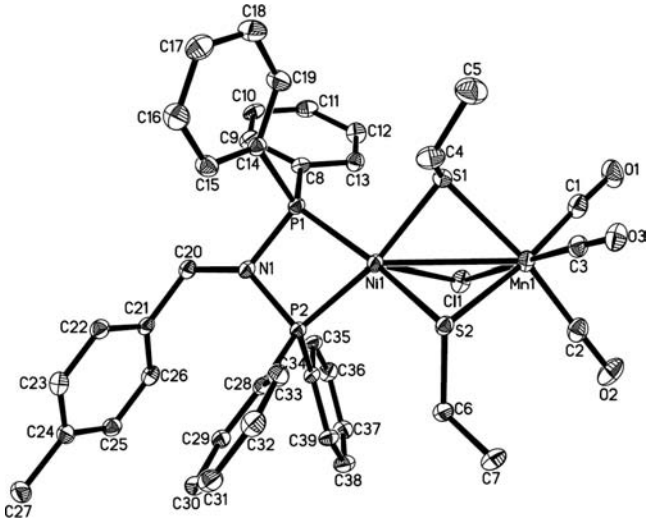

Figure 5. Molecular structure of **7** with 30% probability level ellipsoids. Hydrogen atoms are omitted for clarity.

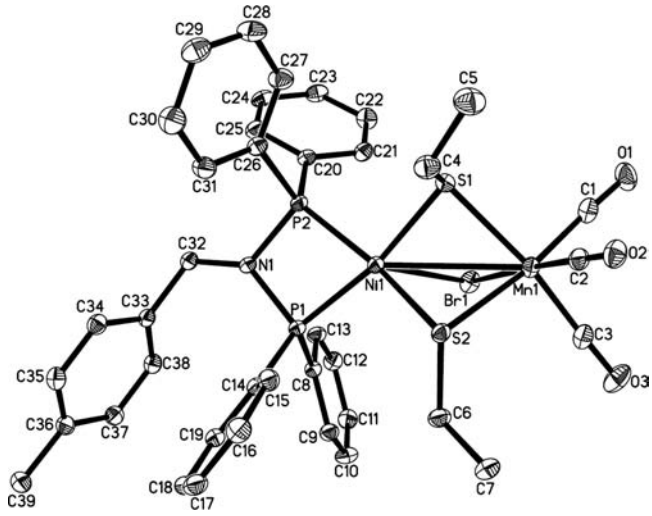

Figure 6. Molecular structure of **9** with 30% probability level ellipsoids. Hydrogen atoms are omitted for clarity.

dx.doi.org/10.1021/ic401978h | *Inorg. Chem.* 2013, 52, 11618−11626

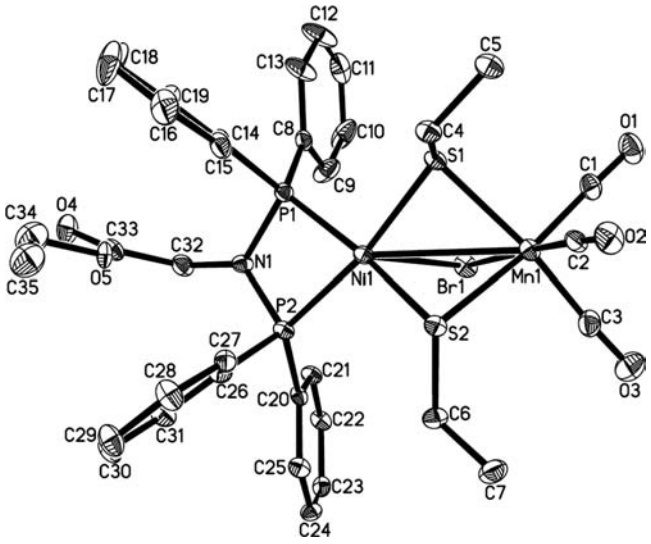

Figure 7. Molecular structure of **10** with 30% probability level ellipsoids. Hydrogen atoms are omitted for clarity.

Table 3. Selected Bond Lengths [Å] and Angles [deg] for Complexes 7, 9, and 10

7			
Ni(1)−P(1)	2.1457(16)	Mn(1)−S(2)	2.3782(13)
Ni(1)−P(2)	2.1655(14)	Mn(1)−S(1)	2.3982(15)
Ni(1)−S(1)	2.2266(15)	Mn(1)−Cl(1)	2.4298(14)
Ni(1)−Cl(1)	2.6613(15)	Ni(1)−Mn(1)	3.0540(19)
P(1)−Ni(1)−P(2)	73.58(6)	P(1)−Ni(1)−Mn(1)	140.93(4)
Mn(1)−Cl(1)−Ni(1)	73.56(5)	S(2)−Mn(1)−S(1)	78.35(5)
S(1)−Ni(1)−S(2)	85.29(5)	S(2)−Mn(1)−Cl(1)	86.85(5)
P(1)−Ni(1)−Cl(1)	112.39(4)	S(1)−Mn(1)−Cl(1)	83.40(6)
9			
Ni(1)−P(1)	2.1637(9)	Mn(1)−S(2)	2.3733(9)
Ni(1)−S(1)	2.2188(9)	Mn(1)−S(1)	2.3899(10)
Ni(1)−Br(1)	2.7955(7)	Mn(1)−Br(1)	2.5697(7)
Ni(1)−Mn(1)	3.0722(9)	P(1)−N(1)	1.705(2)
S(1)−Ni(1)−Br(1)	82.67(2)	Br(1)−Ni(1)−Mn(1)	51.683(12)
P(2)−Ni(1)−P(1)	73.50(3)	S(2)−Mn(1)−S(1)	77.89(3)
P(1)−Ni(1)−Mn(1)	139.93(3)	S(1)−Mn(1)−Br(1)	84.58(3)
P(1)−Ni(1)−S(1)	169.45(3)	S(1)−Mn(1)−Ni(1)	45.86(2)
10			
Br(1)−Mn(1)	2.5672(10)	Ni(1)−Mn(1)	3.0600(11)
Br(1)−Ni(1)	2.7968(9)	Ni(1)−S(1)	2.2417(14)
Ni(1)−P(1)	2.1551(14)	Mn(1)−S(1)	2.3890(15)
Ni(1)−P(2)	2.1820(14)	Mn(1)−S(2)	2.3906(15)
P(1)−Ni(1)−S(1)	96.48(5)	S(1)−Ni(1)−Mn(1)	50.74(4)
P(1)−Ni(1)−Mn(1)	137.44(4)	Br(1)−Ni(1)−Mn(1)	51.76(2)
Mn(1)−Br(1)−Ni(1)	69.41(3)	S(1)−Mn(1)−S(2)	78.90(5)
P(1)−Ni(1)−Br(1)	103.32(4)	S(1)−Mn(1)−Br(1)	83.20(4)

Electrochemical Study on Ni/Mn Model Complexes 7−10. The electrochemical properties of some Ni/Fe[28,38,45,46] and Ni/Ru[29−32] model complexes have been well-studied. Recently, Artero and co-workers reported the electrochemical properties of the first Ni/Mn model complex $[Ni(xbsms)Mn(CO)_3(H_2O)]^+Br^-$ along with its synthesis.[36] The cyclic voltammograms of the new type of Ni/Mn model complexes **7−10** were determined by using *n*-Bu_4NPF_6 as electrolyte in MeCN at a scan rate of 100 mV s^{-1}. While their cyclic voltammograms are shown in Figure 8, Table 4 lists the

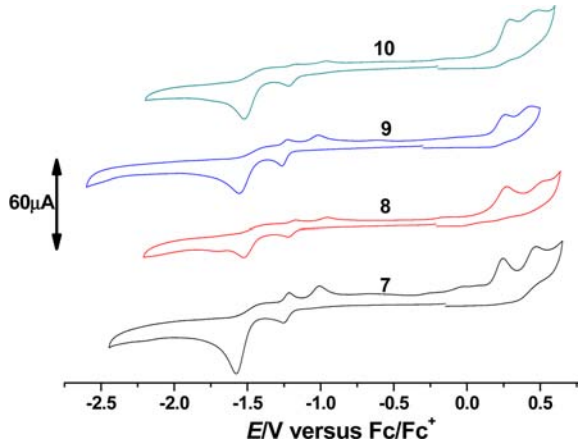

Figure 8. Cyclic voltammograms of **7−10** (1.0 mM) in 0.1 M *n*-Bu_4NPF_6/MeCN at a scan rate of 0.1 V s^{-1}.

Table 4. Electrochemical Data of 7−10

	E_{pc1}/V	E_{pc2}/V	E_{pa1}/V	E_{pa2}/V
7	−1.26	−1.58	0.24	0.47
8	−1.22	−1.52	0.28	0.53
9	−1.25	−1.56	0.26	0.44
10	−1.21	−1.51	0.30	0.49

corresponding electrochemical data. As can be seen in Figure 8 and Table 4, complexes **7−10** each display one quasireversible reduction wave in the range from −1.21 to −1.26 V and one irreversible reduction wave in the range from −1.51 to −1.58 V, respectively. That is, the two reduction waves displayed by **7−10** in MeCN are considerably shifted positively relative to those two waves (−1.53 and −1.83 V) displayed by Artero's complex $[Ni(xbsms)Mn(CO)_3(H_2O)]^+Br^-$ in DMF.[36] It is interesting to note that the first and second reduction waves of the *p*-$MeC_6H_4CH_2$-substituted complexes **7** and **9** are negatively shifted up to 40−60 mV relative to those of the EtO_2CCH_2-substituted complexes **8** and **10**. This is consistent with the observation that *p*-$MeC_6H_4CH_2$ is a much stronger electron-donating group than EtO_2CCH_2. However, in contrast to this, the first and second reduction waves of the Cl-bridged complexes **7** and **8** are just slightly negatively shifted by 10−20 mV relative to those of their Br-bridged analogues **9** and **10**. Apparently, this implies that the bridging chloro and bromo ligands in **7−10** just have a minor influence upon their cyclic voltammetric behavior.

In order to test if the new type of Ni/Mn model complexes **7−10** could act as electrocatalysts for proton reduction to hydrogen, we chose **7** and **9** as representatives to study their electrocatalytic behavior in the presence and absence (for comparison) of HOAc under CV conditions. As shown in Figures 9 and 10, when the first portion of 2 mM acetic acid is added to the MeCN solution of **7** or **9**, the current heights of their original two reduction peaks in the absence of HOAc are slightly increased, but they do not continue to increase with sequential addition of the acid. However, to our surprise, when the first portion of 2 mM HOAc is added, a new irreversible reduction peak at −1.80 V for **7** or −1.79 V for **9** appears, and this reduction peak continues to grow with increase of the acid concentration. In fact, such an observation is consistent with the previously reported electrocatalytic proton reduction processes.[28−32,45,46] As we know, the catalytic efficiency is closely related to the overpotential for a catalytic reaction; in

dx.doi.org/10.1021/ic401978h | *Inorg. Chem.* 2013, 52, 11618−11626

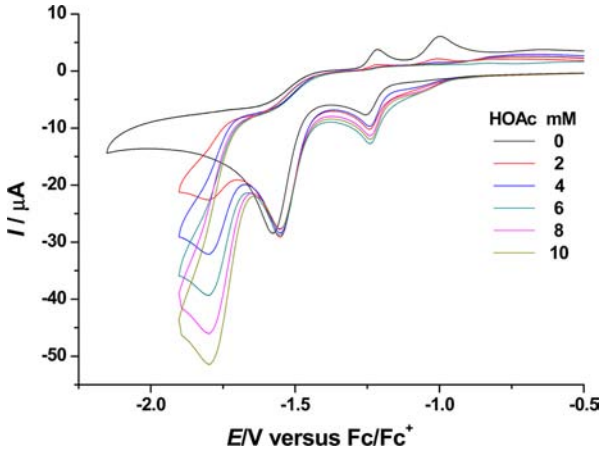

Figure 9. Cyclic voltammograms of **7** (1.0 mM) with HOAc (0−10 mM) in 0.1 M n-Bu_4NPF_6/MeCN at a scan rate of 0.1 V s^{-1}.

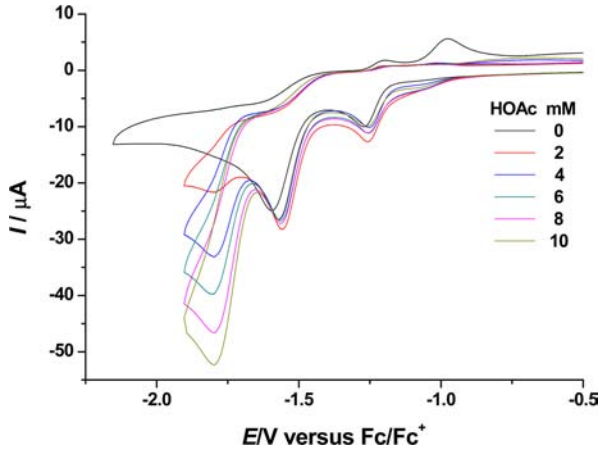

Figure 10. Cyclic voltammograms of **9** (1.0 mM) with HOAc (0−10 mM) in 0.1 M n-Bu_4NPF_6/MeCN at a scan rate of 0.1 V s^{-1}.

addition, the overpotential is equal to the difference between the potential at the half-maximum of the catalytic current and the standard reduction potential ($E°$) of the acid in MeCN.[47−49] Since the $E°$ of acetic acid in MeCN is known to be −1.46 V[49] and the half-wave potentials of **7** and **9** were measured to be 1.73 and 1.72 V, the overpotentials for H_2 production catalyzed by **7** and **9** from HOAc can be calculated as 270 and 260 mV, respectively. It follows that the overpotentials for **7** and **9** are 40 and 50 mV less than that (310 mV) for model complex $[(dppe)Ni(\mu\text{-}pdt)(\mu\text{-}H)Fe(CO)_3][BF_4]$, respectively.[46] Since the overpotential (860 mV) for Artero's complex $[Ni(xbsms)Mn(CO)_3(H_2O)]^+Br^-$ was obtained by the first "derivative" technique method,[36,50] in order to make a fair comparison, we calculated the overpotentials for our Ni/Mn model complexes **7** and **9** to be 470 and 480 mV by using the same method (Supporting Information Figure S1). Thus, the overpotentials for **7** and **9** are 380 and 390 mV less than that for Artero's complex. However, the catalytic current enhancement i_{cat}/i_0 for complexes **7** and **9** (Supporting Information Figure S2) is somewhat less than that for Artero's complex.[36] It is noteworthy that the small overpotentials for our Ni/Mn complexes **7** and **9** as compared to that for Artero's Ni/Mn complex are presumably due to **7** and **9** having an azadiphosphine-chelated Ni moiety {note that the azadiphosphine-chelated mononuclear Ni complex $[Ni(P^{Ph}{}_2N^{C6H4X}{}_2)_2](BF_4)_2$ (X = CF_3) also has a very low overpotential (230 mV)}.[51]

The electrocatalytic H_2 production catalyzed by **7** and **9** were further confirmed by bulk electrolysis. When bulk electrolysis of a MeCN solution of **7** or **9** (0.5 mM) with excess HOAc (25 mM) was carried out at −1.85 V for 0.5 h, a total of 20.9 F mol^{-1} of **7** or 18.2 F mol^{-1} of **9** passed, which corresponds to 10.5 and 9.1 turnovers, respectively. Gas chromatographic analysis showed that the yields of H_2 evolved in the two cases are all about 90%.

CONCLUSIONS

On the basis of preparing the six precursor compounds **1**−**6**, we have successfully synthesized the four Ni/Mn model complexes **7**−**10**. All the new compounds **1**−**10** have been characterized by elemental analysis and spectroscopy, with some of them characterized further by X-ray crystallography. The X-ray crystallographic study on target model complexes **7**, **9**, and **10** indicates the following: (i) They all contain a butterfly $[NiS_2Mn]$ core, in which the metal Ni center and Mn center are bridged by two ethylthiolates and one chloro or bromo ligand. (ii) While each Ni center has a distorted square-pyramidal geometry and is coordinated (except the three bridging ligands) by an additional azadiphosphine ligand **1** or **2**, the Mn center possesses a distorted octahedral geometry and is coordinated by another three terminal CO ligands. (iii) Each of the three model complexes includes a $Mn^{+I}(CO)_3$ (d^6ML_3) fragment that is isolobal with the fragment $Fe^{+II}(CO)(CN)_2$ (d^6ML_3) found in the active site of [NiFe]-hydrogenases. In addition, the representative model complexes **7** and **9** have been found to be catalysts for HOAc proton reduction to H_2 under electrochemical conditions. It follows that complexes **7**−**10** are not only good structural models, but also the functional models for the active site of [NiFe]-hydrogenases. To the best of our knowledge, complexes **7**−**10** are the first examples of the neutral Ni/Mn model complexes, although the first cationic type of Ni/Mn model complex $[Ni(xbsms)Mn(CO)_3(H_2O)]^+Br^-$ was previously reported.[36]

EXPERIMENTAL SECTION

General Comments. All reactions were carried out using standard Schlenk or vacuum-line techniques under an atmosphere of prepurified nitrogen. Ph_2PCl, p-methylbenzylamine, glycine ethyl ester hydrochloride ($EtO_2CCH_2NH_2{\cdot}HCl$), $NiCl_2{\cdot}6H_2O$, EtSH, $Mn(CO)_5Br$, and other chemicals were available commercially and used as received, while $Mn(CO)_5Cl$ was prepared according to the literature procedures.[52] IR spectra were recorded on a Bio-Rad FTS 6000 spectrophotometer. ^1H NMR, $^{13}C\{H\}$ NMR, and $^{31}P\{H\}$ NMR spectra were taken on a Bruker Avance 400 NMR spectrometer. Elemental analysis was performed on an Elementar Vario EL analyzer. Melting points were determined on a SGW X-4 microscopic melting point apparatus and are uncorrected.

Preparation of $RN(PPh_2)_2$ (1, R = p-$MeC_6H_4CH_2$; 2, R = EtO_2CCH_2). To a stirred mixture of p-methylbenzylamine (1.212 g, 10.0 mmol) and Et_3N (4.9 mL, 35.0 mmol) in CH_2Cl_2 (40 mL) was slowly added Ph_2PCl (3.6 mL, 20.0 mmol) at 0 °C. The resulting white suspension was further stirred at room temperature for 12 h and then was washed with saturated sodium hydroxide solution (3 × 20 mL). After the organic layer was dried with anhydrous $MgSO_4$, solvent was removed at reduced pressure to give a yellow viscous solid. Recrystallization of this solid in EtOH afforded diphosphine **1** (1.861 g, 38%) as a white solid, mp 117−119 °C. Anal. Calcd for $C_{32}H_{29}NP_2$: C, 78.51; H, 5.97; N, 2.86. Found: C, 78.36; H, 6.15; N, 3.00. IR (KBr disk): ν_{P-N-P} 834 (s) cm^{-1}. ^1H NMR (400 MHz, DMSO-d_6): 2.17 (s,

dx.doi.org/10.1021/ic401978h | Inorg. Chem. 2013, 52, 11618−11626

Table 5. Crystal Data and Structure Refinements Details for 1−3

	1	2	3
mol formula	$C_{32}H_{29}NP_2$	$C_{28}H_{27}NO_2P_2$	$C_{33}H_{31}Cl_4NNiP_2$
mol wt	489.50	471.45	704.04
cryst syst	monoclinic	monoclinic	monoclinic
space group	$P2_1/n$	$P2_1$	$P2_1/n$
a/Å	8.8369(18)	9.665(4)	20.172(10)
b/Å	9.7566(19)	14.527(5)	8.555(3)
c/Å	30.133(6)	9.866(4)	20.614(10)
α/deg	90.00	90	90
β/deg	93.567(3)	117.471(6)	117.179(6)
γ/deg	90	90	90
V/Å^3	2593.0(9)	1229.0(9)	3164(2)
Z	4	2	4
D_c/g cm^{-3}	1.254	1.274	1.478
abs coeff/mm^{-1}	0.189	0.202	1.077
F(000)	1032	496	1448
index ranges	$-10 \le h \le 11$	$-12 \le h \le 11$	$-26 \le h \le 26$
	$-12 \le k \le 12$	$-19 \le k \le 19$	$-10 \le k \le 11$
	$-39 \le l \le 39$	$-12 \le l \le 12$	$-26 \le l \le 27$
no. reflns	25 786	15 822	31 634
no. indep reflns	6188	5839	7491
$2\theta_{max}$/deg	55.76	55.90	55.80
R	0.0479	0.0263	0.0523
R_w	0.1068	0.0583	0.1488
GOF	1.071	1.042	1.121
largest diff peak, hole/e Å^{-3}	0.351/−0.372	0.169/−0.220	1.116/−1.135

3H, CH_3), 4.41 (t, $^3J_{P-H}$ = 10.8 Hz, 2H, NCH_2), 6.61, 6.87 (dd, J = 7.6 Hz, 4H, C_6H_4), 7.28−7.34 (m, 20H, $4C_6H_5$) ppm. $^{13}C\{^1H\}$ NMR (100 MHz, DMSO-d_6): 20.6 (CH_3), 54.9 (NCH_2), 128.2, 128.4, 128.5, 128.9, 132.2, 132.5, 135.8, 136.5, 138.9, 139.0 (C_6H_4, C_6H_5) ppm. $^{31}P\{^1H\}$ NMR (162 MHz, DMSO-d_6, 85% H_3PO_4): 59.1 (s) ppm.

Similarly, when $EtO_2CCH_2NH_2$·HCl (1.401 g, 10.0 mmol) was used instead of p-$MeC_6H_4CH_2NH_2$, diphosphine **2** (2.508 g, 53%) was obtained as a white solid, mp 137−139 °C. Anal. Calcd for $C_{28}H_{27}NO_2P_2$: C, 71.33; H, 5.77; N, 2.97. Found: C, 71.36; H, 6.00; N, 3.12. IR (KBr disk): $\nu_{C=O}$ 1751 (vs); ν_{P-N-P} 835 (s) cm^{-1}. ^1H NMR (400 MHz, DMSO-d_6): 0.94 (t, J = 7.2 Hz, 3H, OCH_2CH_3), 3.72 (q, J = 7.2 Hz, 2H, OCH_2CH_3), 4.04 (t, $^3J_{P-H}$ = 11.4 Hz, 2H, NCH_2), 7.34 (s, 20H, $4C_6H_5$) ppm. $^{13}C\{^1H\}$ NMR (100 MHz, DMSO-d_6): 14.3 (OCH_2CH_3), 54.0 (NCH_2), 60.7 (OCH_2CH_3), 128.6, 129.5, 132.8, 133.0, 138.8, 139.0 (C_6H_5), 171.1 (CO_2) ppm. $^{31}P\{^1H\}$ NMR (162 MHz, DMSO-d_6, 85% H_3PO_4): 64.4 (s) ppm.

Preparation of p-$MeC_6H_4CH_2N(PPh_2)_2NiCl_2$ (3). To a stirred solution of $NiCl_2·6H_2O$ (0.476 g, 2.0 mmol) in MeOH (20 mL) was added a solution of diphosphine **1** (0.982 g, 2.0 mmol) in CH_2Cl_2 (20 mL) at room temperature. The resulting dark-red mixture continued to be stirred at room temperature for 10 h. Volatiles were removed at reduced pressure, and then the residue was subjected to column chromatography by using CH_2Cl_2 as an eluent to produce mononuclear Ni complex **3** (0.733 g, 59%) as a red solid, mp >250 °C. Anal. Calcd for $C_{32}H_{29}Cl_2NNiP_2$: C, 62.08; H, 4.72; N, 2.26. Found: C, 61.91; H, 4.68; N, 2.43. IR (KBr disk): ν_{P-N-P} 816 (s) cm^{-1}. ^1H NMR (400 MHz, DMSO-d_6): 2.10 (s, 3H, CH_3), 4.13 (d, $^3J_{P-H}$ = 23.6 Hz, 2H, NCH_2), 6.23−6.71 (m, 4H, C_6H_4), 7.15−7.82 (m, 20H, $4C_6H_5$) ppm. $^{13}C\{^1H\}$ NMR (100 MHz, DMSO-d_6): 20.5 (CH_3), 51.1 (NCH_2), 128.6, 128.7, 128.9, 129.1, 130.3, 132.2, 132.8, 133.0, 137.4 (C_6H_4, C_6H_5) ppm. $^{31}P\{^1H\}$ NMR (162 MHz, DMSO-d_6, 85% H_3PO_4): 56.2 (s) ppm.

Preparation of $EtO_2CCH_2N(PPh_2)_2NiCl_2$ (4). To a stirred solution of $NiCl_2·6H_2O$ (0.476 g, 2.0 mmol) in MeOH (20 mL) was added a solution of diphosphine **2** (0.942 g, 2.0 mmol) in CH_2Cl_2 (20 mL) at room temperature. The resulting dark-red mixture continued to be stirred at this temperature for 10 h, and then, the volume was concentrated to ca. 5 mL at reduced pressure. Addition of Et_2O (50 mL) gave red precipitates, which were collected by filtration,

Table 6. Crystal Data and Structure Refinements Details for 7, 9, and 10

	7	9	10
mol formula	$C_{39}H_{39}ClMnNNiO_3P_2S_2$	$C_{39}H_{39}BrMnNNiO_3P_2S_2$	$C_{35}H_{37}BrMnNNiO_5$
mol wt	844.87	889.33	939.84
cryst syst	monoclinic	monoclinic	triclinic
space group	$P2_1/n$	$P2_1/n$	$P\bar{1}$
a/Å	11.975(8)	11.995(3)	9.5722(17)
b/Å	17.729(9)	17.737(4)	13.933(2)
c/Å	18.711(12)	18.622(4)	17.134(2)
α/deg	90	90	69.068(14)
β/deg	98.774(10)	99.098(3)	78.86(2)
γ/deg	90	90	84.86(2)
V/Å^3	3926(4)	3912.1(15)	2093.6(6)
Z	4	4	2
D_c/g cm^{-3}	1.429	1.510	1.491
abs coeff/mm^{-1}	1.095	2.051	1.961
F(000)	1744	1816	963
index ranges	$-15 \le h \le 15$	$-15 \le h \le 15$	$-11 \le h \le 11$
	$-23 \le k \le 23$	$-23 \le k \le 23$	$-16 \le k \le 16$
	$-24 \le l \le 24$	$-24 \le l \le 23$	$-19 \le l \le 20$
no. reflns	49 242	39 505	18 631
no. indep reflns	9303	9277	7368
$2\theta_{max}$/deg	55.74	55.74	50.04
R	0.0568	0.0471	0.0581
R_w	0.1353	0.1143	0.1375
GOF	1.148	1.076	1.069
largest diff peak, hole/e Å^{-3}	1.395/−0.621	1.390/−0.706	1.195/−0.772

dx.doi.org/10.1021/ic401978h | Inorg. Chem. 2013, 52, 11618−11626

washed with Et_2O (3 × 5 mL), and finally dried under vacuum. The mononuclear Ni complex **4** (0.937 g, 78%) was obtained as a red solid, mp 232−234 °C. Anal. Calcd for $C_{28}H_{27}Cl_2NNiO_2P_2$: C, 55.95; H, 4.53; N, 2.33. Found: C, 56.05; H, 4.59; N, 2.34. IR (KBr disk): $\nu_{C=O}$ 1731 (vs); ν_{P-N-P} 810 (s) cm^{-1}. ^1H NMR (400 MHz, $CDCl_3$): 0.87 (t, J = 6.8 Hz, 3H, OCH_2CH_3), 3.41 (t, $^3J_{P-H}$ = 12.6 Hz, 2H, NCH_2), 3.64 (q, J = 6.8 Hz, 2H, OCH_2CH_3), 7.52−8.04 (m, 20H, $4C_6H_5$) ppm. $^{13}C\{^1H\}$ NMR (100 MHz, $CDCl_3$): 13.6 (OCH_2CH_3), 48.0 (NCH_2), 61.8 (OCH_2CH_3), 126.7, 129.3, 133.2, 133.6 (C_6H_5), 166.9 (CO_2) ppm. $^{31}P\{^1H\}$ NMR (162 MHz, $CDCl_3$, 85% H_3PO_4): 46.7 (s) ppm.

Preparation of $RN(PPh_2)_2Ni(SEt)_2$ (5, R = *p*-$MeC_6H_4CH_2$; 6, R = EtO_2CCH_2). To a stirred solution of **3** (3.096 g, 5.0 mmol) and EtSH (0.621 g, 10.0 mmol) in CH_2Cl_2 (50 mL) was slowly added Et_3N (3.9 mL, 28.0 mmol) at room temperature, and then the new mixture was stirred for an additional 1 h at this temperature. Solvent was removed at reduced pressure, and the residue was washed successively with water (3 × 50 mL), methanol (3 × 10 mL), and diethyl ether (3 × 10 mL), and finally dried under vacuum. Mononuclear Ni complex **5** (2.146 g, 64%) was obtained as a green solid, mp 135−137 °C. Anal. Calcd for $C_{36}H_{39}NNiP_2S_2$: C, 64.49; H, 5.86; N, 2.09. Found: C, 64.37; H, 5.86; N, 2.34. IR (KBr disk): ν_{P-N-P} 808 (s) cm^{-1}. ^1H NMR (400 MHz, $CDCl_3$): 1.01 (br s, 6H, $2SCH_2CH_3$), 2.15 (s, 3H, $C_6H_4CH_3$), 2.22 (br s, 4H, $2SCH_2CH_3$), 3.83 (br s, 2H, NCH_2), 6.19, 6.60 (2br s, 4H, C_6H_4), 7.40−7.91 (m, 20H, $4C_6H_5$) ppm. $^{13}C\{^1H\}$ NMR (100 MHz, $CDCl_3$): 19.5 (SCH_2CH_3), 20.9 ($C_6H_4CH_3$), 23.2 (SCH_2CH_3), 51.6 (NCH_2), 128.7, 128.9, 129.1, 129.3, 129.5, 131.7, 133.8, 137.5 (C_6H_4, C_6H_5) ppm. $^{31}P\{^1H\}$ NMR (162 MHz, $CDCl_3$, 85% H_3PO_4): 60.4 (s) ppm.

Similarly, when **4** (3.005 g, 5.0 mmol) was used in place of **3**, mononuclear Ni complex **6** (2.218 g, 68%) was obtained as a yellow solid, mp >250 °C. Anal. Calcd for $C_{32}H_{37}NNiO_2P_2S_2$: C, 58.91; H, 5.72; N, 2.15. Found: C, 58.78; H, 5.83; N, 2.28. IR (KBr disk): $\nu_{C=O}$ 1745 (vs); ν_{P-N-P} 831 (s) cm^{-1}. ^1H NMR (400 MHz, $CDCl_3$): 0.82 (br s, 3H, OCH_2CH_3), 1.03 (br s, 6H, $2SCH_2CH_3$), 2.24 (br s, 4H, $2SCH_2CH_3$), 3.34 (t, $^3J_{P-H}$ = 11.2 Hz, 2H, NCH_2), 3.52 (br s, 2H, OCH_2CH_3), 7.48−8.00 (m, 20H, $4C_6H_5$) ppm. $^{13}C\{^1H\}$ NMR (100 MHz, $CDCl_3$): 13.5 (OCH_2CH_3), 19.4 (SCH_2CH_3), 23.4 (SCH_2CH_3), 48.2 (NCH_2), 61.3 (OCH_2CH_3), 128.8, 132.2, 133.0, 133.9 (C_6H_5), 167.6 (CO_2) ppm. $^{31}P\{^1H\}$ NMR (162 MHz, $CDCl_3$, 85% H_3PO_4): 62.9 (s) ppm.

Preparation of $RN(PPh_2)_2Ni(\mu\text{-}SEt)_2(\mu\text{-}Cl)Mn(CO)_3$ (7, R = *p*-$MeC_6H_4CH_2$; 8, R = EtO_2CCH_2). $Mn(CO)_5Cl$ (0.173 g, 0.75 mmol) was added to a stirred solution of **5** (0.503 g, 0.75 mmol) in CH_2Cl_2 (50 mL). The reaction mixture was stirred for 3 days at room temperature. Volatiles were removed at reduced pressure, and then the residue was subjected to column chromatography by using CH_2Cl_2/MeOH (100:1 v/v) as eluent to give dinuclear Ni/Mn complex **7** (0.463 g, 73%) as a brown solid, mp 178−180 °C. Anal. Calcd for $C_{39}H_{39}ClMnNNiO_3P_2S_2$: C, 55.44; H, 4.65; N, 1.66. Found: C, 55.66; H, 4.72; N, 1.53. IR (KBr disk): $\nu_{C\equiv O}$ 2000 (vs), 1904 (vs), 1883 (vs); ν_{P-N-P} 818 (s) cm^{-1}. ^1H NMR (400 MHz, $CDCl_3$): 1.02 (s, 6H, $2SCH_2CH_3$), 2.00−2.25 (m, 7H, $C_6H_4CH_3$, $2SCH_2CH_3$), 3.71 (br s, 2H, NCH_2), 6.15, 6.60 (2s, 4H, C_6H_4), 7.45−7.92 (m, 20H, $4C_6H_5$) ppm. $^{13}C\{^1H\}$ NMR (100 MHz, $CDCl_3$): 17.0 (SCH_2CH_3), 20.9 ($C_6H_4CH_3$), 27.9 (SCH_2CH_3), 51.5 (NCH_2), 128.9, 131.4, 132.1, 132.7, 133.5, 137.7 (C_6H_4, C_6H_5), 219.8, 225.5 ($C_{\equiv}O$) ppm. $^{31}P\{^1H\}$ NMR (162 MHz, $CDCl_3$, 85% H_3PO_4): 44.5 (s) ppm.

Similarly, when **6** (0.489 g, 0.75 mmol) was employed in place of **5**, dinuclear Ni/Mn complex **8** (0.223 g, 36%) was obtained as a brown solid, mp 86−88 °C. Anal. Calcd for $C_{35}H_{37}ClMnNNiO_5P_2S_2$: C, 50.84; H, 4.51; N, 1.69. Found: C, 50.94; H, 4.39; N, 1.98. IR (KBr disk): $\nu_{C\equiv O}$ 2004 (vs), 1903 (vs); $\nu_{C=O}$ 1740 (s); ν_{P-N-P} 813 (s) cm^{-1}. ^1H NMR (400 MHz, $CDCl_3$): 0.81−1.03 (m, 9H, OCH_2CH_3, $2SCH_2CH_3$), 2.04 (br s, 4H, $2SCH_2CH_3$), 3.25 (br.s, 2H, NCH_2), 3.56 (br s, 2H, OCH_2CH_3), 7.50−8.05 (m, 20H, $4C_6H_5$) ppm. $^{13}C\{^1H\}$ NMR (100 MHz, $CDCl_3$): 13.5 (OCH_2CH_3), 16.9 (SCH_2CH_3), 28.0 (SCH_2CH_3), 47.9 (NCH_2), 61.4 (OCH_2CH_3), 129.1, 132.6, 133.1, 133.6 (C_6H_5), 167.4 (CO_2), 219.8, 225.5 ($C_{\equiv}O$) ppm. $^{31}P\{^1H\}$ NMR (162 MHz, $CDCl_3$, 85% H_3PO_4): 46.8 (s) ppm.

Preparation of $RN(PPh_2)_2Ni(\mu\text{-}SEt)_2(\mu\text{-}Br)Mn(CO)_3$ (9, R = *p*-$MeC_6H_4CH_2$; 10, R = EtO_2CCH_2). To a stirred solution of **5** (0.503 g, 0.75 mmol) in CH_2Cl_2 (50 mL) was added $Mn(CO)_5Br$ (0.206 g, 0.75 mmol) at room temperature, and then the mixture was stirred for 3 days at this temperature. Volatiles were removed at reduced pressure to give a residue, which was subjected to column chromatography by using CH_2Cl_2 as an eluent to afford dinuclear Ni/Mn complex **9** (0.334 g, 50%) as a brown solid, mp 192−194 °C. Anal. Calcd for $C_{39}H_{39}BrMnNNiO_3P_2S_2$: C, 52.67; H, 4.42; N, 1.57. Found: C, 52.39; H, 4.44; N, 1.85. IR (KBr disk): $\nu_{C\equiv O}$ 2000 (vs), 1904 (vs); ν_{P-N-P} 816 (s) cm^{-1}. ^1H NMR (400 MHz, $CDCl_3$): 1.03 (br s, 6H, $2SCH_2CH_3$), 1.90−2.25 (m, 7H, $C_6H_4CH_3$, $2SCH_2CH_3$), 3.72 (br s, 2H, NCH_2), 6.14, 6.60 (2s, 4H, C_6H_4), 7.40−8.20 (m, 20H, $4C_6H_5$) ppm. $^{13}C\{^1H\}$ NMR (100 MHz, $CDCl_3$): 16.8 (SCH_2CH_3), 20.9 ($C_6H_4CH_3$), 29.2 (SCH_2CH_3), 51.5 (NCH_2), 128.9, 129.0, 131.5, 132.1, 134.2, 137.8 (C_6H_4, C_6H_5), 219.8, 226.7 ($C_{\equiv}O$) ppm. $^{31}P\{^1H\}$ NMR (162 MHz, $CDCl_3$, 85% H_3PO_4): 51.7 (s) ppm.

Similarly, when **6** (0.489 g, 0.75 mmol) was utilized instead of **5**, dinuclear Ni/Mn complex **10** (0.202 g, 31%) was obtained as a brown solid, mp 172−174 °C. Anal. Calcd for $C_{35}H_{37}BrMnNNiO_5P_2S_2$: C, 48.25; H, 4.28; N, 1.61. Found: C, 48.15; H, 4.30; N, 1.79. IR (KBr disk): $\nu_{C\equiv O}$ 2001 (vs), 1900 (vs); $\nu_{C=O}$ 1743 (s); ν_{P-N-P} 815 (s) cm^{-1}. ^1H NMR (400 MHz, $CDCl_3$): 0.84 (s, 3H, OCH_2CH_3), 1.03 (s, 6H, $2SCH_2CH_3$), 2.06 (br s, 4H, $2SCH_2CH_3$), 3.26 (br s, 2H, NCH_2), 3.56 (br s, 2H, OCH_2CH_3), 7.40−8.25 (m, 20H, $4C_6H_5$) ppm. $^{13}C\{^1H\}$ NMR (100 MHz, $CDCl_3$): 13.5 (OCH_2CH_3), 16.8 (SCH_2CH_3), 29.3 (SCH_2CH_3), 47.8 (NCH_2), 61.4 (OCH_2CH_3), 126.8, 129.0, 132.6, 134.4 (C_6H_5), 167.4 (CO_2), 219.7, 226.7 ($C_{\equiv}O$) ppm. $^{31}P\{^1H\}$ NMR (162 MHz, $CDCl_3$, 85% H_3PO_4): 54.3 (s) ppm.

X-ray Structure Determinations of 1−3, 7, 9, and 10. The single crystals suitable for X-ray diffraction analysis were grown by the slow evaporation of CH_2Cl_2/*n*-hexane solution of **1**−**3**, **7**, **9**, and **10** at room temperature. Each crystal was mounted on a Rigaku MM-007 (rotating anode) diffractometer equipped with Saturn 724 CCD. Data were collected at 113(2) K using a confocal monochromator with Mo Kα radiation (λ = 0.710 73 Å) in the $\omega-\phi$ scanning mode. Data collection, reduction, and absorption correction were performed by CRYSTALCLEAR program.[53] The structures were solved by direct methods using the SHELXS-97 program[54] and refined by full-matrix least-squares techniques (SHELXL-97)[55] on F^2. Hydrogen atoms were located by using the geometric method. Details of crystal data, data collections, and structure refinements are summarized in Tables 5 and 6.

Electrochemical and Eelectrocatalytic Experiments. A solution of 0.1 M *n*-Bu_4NPF_6 in MeCN (Fisher Chemicals, HPLC grade) was used as electrolyte in each of electrochemical and electrocatalytic experiments. The electrolyte solutions were degassed by bubbling with N_2 for at least 10 min before measurements. The measurements were made using a BAS Epsilon potentiostat. All voltammograms were obtained in a three-electrode cell with a 3 mm diameter glassy carbon working electrode, a platinum counter electrode, and a Ag/Ag^+ (0.01 M $AgNO_3$/0.1 M *n*-Bu_4NPF_6 in MeCN) reference electrode under an atmosphere of nitrogen. The working electrode was polished with 0.05 μm alumina paste and sonicated in water for 10 min. Bulk electrolyses were run on a vitreous carbon rod (A = 2.9 cm^2) in a two-compartment, gas-tight, H-type electrolysis cell containing ca. 10 mL of MeCN. All potentials are quoted against Fc/Fc^+ potential. Gas chromatography was performed with a Shimadzu gas chromatograph GC-2014 under isothermal conditions with nitrogen as a carrier gas and a thermal conductivity detector.

■ ASSOCIATED CONTENT

Ⓢ Supporting Information

Figures S1 and S2. Full tables of crystal data, atomic coordinates and thermal parameters, and bond lengths and angles for **1**−**3**, **7**, **9**, and **10** as CIF files. This material is available free of charge via the Internet at http://pubs.acs.org.

AUTHOR INFORMATION

Corresponding Author

*E-mail: lcsong@nankai.edu.cn.

Notes

The authors declare no competing financial interest.

ACKNOWLEDGMENTS

We are grateful to the National Natural Science Foundation of China (21132001, 21272122), 973 (2011CB935902), and Synergetic Innovation Center of Chemical Science and Engineering (Tianjin) for financial support.

REFERENCES

(1) Cammack, R. *Nature* **1999**, *397*, 214−215.
(2) Adams, M. W. W.; Stiefel, E. I. *Science* **1998**, *282*, 1842−1843.
(3) Evans, D. J.; Pickett, C. J. *Chem. Soc. Rev.* **2003**, *32*, 268−275.
(4) Frey, M. *ChemBioChem* **2002**, *3*, 153−160.
(5) Lubitz, W.; Reijerse, E.; van Gastel, M. *Chem. Rev.* **2007**, *107*, 4331−4365.
(6) (a) Fontecilla-Camps, J. C.; Volbeda, A.; Cavazza, C.; Nicolet, Y. *Chem. Rev.* **2007**, *107*, 4273−4303. (b) Bouwman, E.; Reedijk, J. *Coord. Chem. Rev.* **2005**, *249*, 1555−1581.
(7) Shima, S.; Thauer, R. K. *Chem. Rec.* **2007**, *7*, 37−46.
(8) Dey, S.; Das, P. K.; Dey, A. *Coord. Chem. Rev.* **2013**, *257*, 42−63.
(9) (a) Ogata, H.; Hirota, S.; Nakahara, A.; Komori, H.; Shibata, N.; Kato, T.; Kano, K.; Higuchi, Y. *Structure* **2005**, *13*, 1635−1642. (b) Volbeda, A.; Garcin, E.; Piras, C.; de Lacey, A. L.; Fernandez, V. M.; Hatchikian, E. C.; Frey, M.; Fontecilla-Camps, J. C. *J. Am. Chem. Soc.* **1996**, *118*, 12989−12996.
(10) Higuchi, Y.; Yagi, T.; Yasuoka, N. *Structure* **1997**, *5*, 1671−1680.
(11) Higuchi, Y.; Ogata, H.; Miki, K.; Yasuoka, N.; Yagi, T. *Structure* **1999**, *7*, 549−556.
(12) Garcin, E.; Vernede, X.; Hatchikian, E. C.; Volbeda, A.; Frey, M.; Fontecilla-Camps, J. C. *Structure* **1999**, *7*, 557−566.
(13) Happe, R. P.; Roseboom, W.; Pierik, A. J.; Albracht, S. P. J.; Bagley, K. A. *Nature* **1997**, *385*, 126.
(14) Fontecilla-Camps, J. C.; Frey, M.; Garcin, E.; Hatchikian, C.; Montet, Y.; Piras, C.; Vernède, X.; Volbeda, A. *Biochimie* **1997**, *79*, 661−666.
(15) Tard, C.; Pickett, C. J. *Chem. Rev.* **2009**, *109*, 2245−2274.
(16) Sellmann, D.; Geipel, F.; Lauderbach, F.; Heinemann, F. W. *Angew. Chem., Int. Ed.* **2002**, *41*, 632−634.
(17) Smith, M. C.; Barclay, J. E.; Cramer, S. P.; Davies, S. C.; Gu, W.-W.; Hughes, D. L.; Longhurst, S.; Evans, D. J. *J. Chem. Soc., Dalton Trans.* **2002**, 2641−2647.
(18) Li, Z.; Ohki, Y.; Tatsumi, K. *J. Am. Chem. Soc.* **2005**, *127*, 8950−8951.
(19) Stenson, P. A.; Marin-Becerra, A.; Wilson, C.; Blake, A. J.; McMaster, J.; Schröder, M. *Chem. Commun.* **2006**, 317−319.
(20) Ohki, Y.; Yasumura, K.; Kuge, K.; Tanino, S.; Ando, M.; Li, Z.; Tatsumi, K. *Proc. Natl. Acad. Sci. U.S.A.* **2008**, *105*, 7652−7657.
(21) Zhu, W.; Marr, A. C.; Wang, Q.; Neese, F.; Spencer, D. J. E.; Blake, A. J.; Cooke, P. A.; Wilson, C.; Schröder, M. *Proc. Natl. Acad. Sci. U.S.A.* **2005**, *102*, 18280−18285.
(22) Schilter, D.; Nilges, M. J.; Chakrabarti, M.; Lindahl, P. A.; Rauchfuss, T. B.; Stein, M. *Inorg. Chem.* **2012**, *51*, 2338−2348.
(23) Jiang, J.; Maruani, M.; Solaimanzadeh, J.; Lo, W.; Koch, S. A.; Millar, M. *Inorg. Chem.* **2009**, *48*, 6359−6361.
(24) Ohki, Y.; Yasumura, K.; Ando, M.; Shimokata, S.; Tatsumi, K. *Proc. Natl. Acad. Sci. U.S.A.* **2010**, *107*, 3994−3997.
(25) Ohki, Y.; Tatsumi, K. *Eur. J. Inorg. Chem.* **2011**, 973−985.
(26) Ogo, S.; Ichikawa, K.; Kishima, T.; Matsumoto, T.; Nakai, H.; Kusaka, K.; Ohhara, T. *Science* **2013**, *339*, 682−684.
(27) Schilter, D.; Rauchfuss, T. B.; Stein, M. *Inorg. Chem.* **2012**, *51*, 8931−8941.
(28) Barton, B. E.; Whaley, C. M.; Rauchfuss, T. B.; Gray, D. L. *J. Am. Chem. Soc.* **2009**, *131*, 6942−6943.
(29) Canaguier, S.; Vaccaro, L.; Artero, V.; Ostermann, R.; Pécaut, J.; Field, M. J.; Fontecave, M. *Chem.—Eur. J.* **2009**, *15*, 9350−9364.
(30) Oudart, Y.; Artero, V.; Norel, L.; Train, C.; Pécaut, J.; Fontecave, M. *J. Organomet. Chem.* **2009**, *694*, 2866−2869.
(31) Oudart, Y.; Artero, V.; Pécaut, J.; Lebrun, C.; Fontecave, M. *Eur. J. Inorg. Chem.* **2007**, 2613−2626.
(32) Oudart, Y.; Artero, V.; Pécaut, J.; Fontecave, M. *Inorg. Chem.* **2006**, *45*, 4334−4336.
(33) Ogo, S.; Kabe, R.; Uehara, K.; Kure, B.; Nishimura, T.; Menon, S. C.; Harada, R.; Fukuzumi, S.; Higuchi, Y.; Ohhara, T.; Tamada, T.; Kuroki, R. *Science* **2007**, *316*, 585−587.
(34) Ichikawa, K.; Matsumoto, T.; Ogo, S. *Dalton Trans.* **2009**, 4304−4309.
(35) Razavet, M.; Artero, V.; Cavazza, C.; Oudart, Y.; Lebrun, C.; Fontecilla-Camps, J. C.; Fontecave, M. *Chem. Commun.* **2007**, 2805−2807.
(36) Fourmond, V.; Canaguier, S.; Golly, B.; Field, M. J.; Fontecave, M.; Artero, V. *Energy Environ. Sci.* **2011**, *4*, 2417−2427.
(37) Song, L.-C.; Li, Y.-L.; Li, L.; Gu, Z.-C.; Hu, Q.-M. *Inorg. Chem.* **2010**, *49*, 10174−10182.
(38) Song, L.-C.; Sun, X.-J.; Zhao, P.-H.; Li, J.-P.; Song, H.-B. *Dalton Trans.* **2012**, *41*, 8941−8950.
(39) Hoffmann, R. *Angew. Chem., Int. Ed.* **1982**, *21*, 711−724.
(40) Helm, M. L.; Stewart, M. P.; Bullock, R. M.; DuBois, M. R.; DuBois, D. L. *Science* **2011**, *333*, 863−866.
(41) Biricik, N.; Durap, F.; Kayan, C.; Gümgüm, B.; Gürbüz, N.; Özdemir, I.; Ang, W. H.; Fei, Z.; Scopelliti, R. *J. Organomet. Chem.* **2008**, *693*, 2693−2699.
(42) Song, K.; Gao, H.; Liu, F.; Pan, J.; Guo, L.; Zai, S.; Wu, Q. *Eur. J. Inorg. Chem.* **2009**, 3016−3024.
(43) Fei, Z.; Scopelliti, R.; Dyson, P. J. *Dalton Trans.* **2003**, 2772−2779.
(44) Sun, Z.; Zhu, F.; Wu, Q.; Lin, S. *Appl. Organomet. Chem.* **2006**, *20*, 175−180.
(45) Canaguier, S.; Field, M.; Oudart, Y.; Pécaut, J.; Fontecave, M.; Artero, V. *Chem. Commun.* **2010**, *46*, 5876−5878.
(46) Barton, B. E.; Rauchfuss, T. B. *J. Am. Chem. Soc.* **2010**, *132*, 14877−14885.
(47) Harb, M. K.; Windhager, J.; Niksch, T.; Görls, H.; Sakamoto, T.; Smith, E. R.; Glass, R. S.; Lichtenberger, D. L.; Evans, D. H.; El-khateeb, M.; Weigand, W. *Tetrahedron* **2012**, *68*, 10592−10599.
(48) Felton, G. A. N.; Mebi, C. A.; Petro, B. J.; Vannucci, A. K.; Evans, D. H.; Glass, R. S.; Lichtenberger, D. L. *J. Organomet. Chem.* **2009**, *694*, 2681−2699.
(49) Felton, G. A. N.; Glass, R. S.; Lichtenberger, D. L.; Evans, D. H. *Inorg. Chem.* **2006**, *45*, 9181−9184.
(50) Fourmond, V.; Jacques, P.-A.; Fontecave, M.; Artero, V. *Inorg. Chem.* **2010**, *49*, 10338−10347.
(51) Kilgore, U. J.; Roberts, J. A. S.; Pool, D. H.; Appel, A. M.; Stewart, M. P.; DuBois, M. R.; Dougherty, W. G.; Kassel, W. S.; Bullock, R. M.; DuBois, D. L. *J. Am. Chem. Soc.* **2011**, *133*, 5861−5872.
(52) Davis, R.; Durrant, J. L. A.; Rowland, C. C. *J. Organomet. Chem.* **1986**, *315*, 119−133.
(53) *CrystalClear and Crystalstructure*; Rigaku and Rigaku Americas: The Woodlands, TX, 2007.
(54) Sheldrick, G. M. *SHELXS97, A Program for Crystal Structure Solution*; University of Göttingen: Germany, 1997.
(55) Sheldrick, G. M. *SHELXL97, A Program for Crystal Structure Refinement*; University of Göttingen: Germany, 1997.